Eur. Phys. J. B **27**, 467–472 (2002)
DOI: 10.1140/epjb/e2002-00179-8

THE EUROPEAN
PHYSICAL JOURNAL B

Evidence of local structural transition during oxidation process of RBCO epitaxial films using time resolved reflexafs measurements

M. Salluzzo[1,a], F. Natali[2,3], C. Aruta[1,4], M.G. Maglione[1], F. Ricci[1], E. Koller[5], Ø. Fischer[5], and N.L. Saini[6]

[1] INFM and Dipartimento di Scienze Fisiche, Università di Napoli "Federico II", Piazzale Tecchio 80, 80125 Napoli, Italy
[2] Operative Group in Grenoble - IN13, BP 156x, 38042 Grenoble Cedex, France
[3] European Synchrotron Radiation Facility, BP 220, 38043 Grenoble Cedex, France
[4] INFM-Università di Roma "Tor Vergata", Dipartimento di Scienze e Tecnologie Fisiche ed Energetiche, Via di Tor Vergata s.n.c., 00133 Roma, Italy
[5] Département de Physique de la Matière Condensée, Université de Genève, 1211 Genève 4, Switzerland
[6] Dipartimento di Fisica, Università di Roma "La Sapienza", P.le Aldo Moro 2, 00185 Roma, Italy

Received 21 December 2001

Abstract. We report results of a time resolved X-ray Absorption Spectroscopy (XAS) experiment on the oxidation process of epitaxial $Y_1(Nd_{0.05}Ba_{1.95})Cu_3O_x$ superconducting thin films. For the first time Cu K-edge XAS technique has been used to explore local structural changes around the Cu ions during the oxidation process of a high critical temperature superconducting film. The results show that during the oxygenation of a tetragonal $Y_1(Nd_{0.05}Ba_{1.95})Cu_3O_x$ additional local transitions appear in the orthorhombic I phase, which are not linked to long range order transformations as shown by *in situ* X-ray diffraction experiment. New questions concerning the dynamic microscopic process leading to the oxygenation and eventually to superconductivity of the complex $R_{1+x}Ba_{2-x}Cu_3O_x$ (R = Y or rare earth) compounds arose from these results.

PACS. 74.72.Bk Y-based cuprates – 74.76.Bz High-T_c films – 68.55.Ln Defects and impurities: doping, implantation, distribution, concentration, etc. – 78.70.Dm X-ray absorption spectra

Introduction

The performance of microelectronic devices based on high critical temperature superconductors (HT_cS) epitaxial films is highly dependent on their structural and chemical perfection [1,2]. Cationic disorder [3] and oxygen disorder [4] are among the main factors which affect the transport properties of HT_cS films. In the $R_{1+y}Ba_{2-y}Cu_3O_x$ (RBCO, R = rare earth or Y) compounds the critical temperature [5], the critical current density [6], the irreversibility field and the anisotropy [7], are very sensitive to the overall oxygen content and to the disorder in the CuO chains. The RBCO films grown by the physical vapour deposition techniques (PVD), deposited at high temperature in partial oxidizing atmosphere, are tetragonal and insulating with an oxygen content lower than $x = 6.3$. The tetragonal to orthorhombic transition is accomplished by cooling the sample to room temperature in high oxygen pressure (≤760 torr) or by an annealing step at intermediate temperature (500 °C). During this process the oxygen content increases until the superconducting optimally and/or over-doped phases with $x \sim 7.0$ (OI phase) are reached. The optimisation of this annealing step is therefore important and several techniques, such as thermogravimetric analysis (TGA) [8], differential thermal analysis (DTA) [8], X-ray diffraction (XRD) [9], and conductivity measurements [10] have been used to provide detailed information on the underneath physical process. The fundamental phenomenon that determines the oxygenation, is the approaching to the steady thermodynamic structural phase at given pressure-temperature conditions. In the case of single crystals, this process could be relatively slow because the main parameter that determines the rate of oxidation is the diffusion of oxygen in the structure. Since the diffusion along the *c*-axis is negligible [11], the bulk oxygenation is more easily accomplished by the introduction of oxygen through morphological or structural defects such as twin-boundaries [12] and consequent diffusion along the ab-plane.

A relevant question concerns the ordering of the oxygen atoms during the oxidation process. In fact, it is not clear if the inclusion of oxygen is accompanied by intermediate structural transformations through stable and possibly metastable RBCO phases corresponding to different oxygen ordering. This is of particular interest since many

---

[a] e-mail: `salluzzo@na.infn.it`

studies on oxidation of YBCO have pointed out that oxygen ordering rather than overall oxygen content has the important role on the stability and on the superconducting properties of this material. Indeed it has been demonstrated that various oxygen configuration, possibly characterised by different T_c's, can be realised even with the same overall oxygen concentration [13]. However it turns out that these states are quite unstable and difficult to observe, and it is impossible to "freeze" them because even at room temperature substantial diffusion of oxygen leads to stabilisation of other more stable structures [14]. Nevertheless it seems quite important to understand exactly what is the underling process leading to the structural transformation of RBCO material, especially in the case of *in situ* deposited thin films, since oxygen disorder can be frozen on atomic scale, depending on the oxidation process history.

Here we report a direct evidence of local structural changes in the CuO_2 and CuO planes during the oxidation process of epitaxially grown high quality $Y_1(Nd_{0.05}Ba_{1.95})Cu_3O_x$ (YNBCO) superconducting thin films using X-ray Absorption Spectroscopy (XAS). To best of our knowledge, the time resolved X-ray Absorption Near Edge Structure (XANES) spectroscopy has been used for the first time to monitor the evolution of the local structural transformations occurring during the oxygenation of RBCO superconducting thin films. XANES spectroscopy is very sensitive to any small change in the local atomic distribution, being a probe of higher order pair distribution function, and well suited for the present work. Other techniques generally employed to study the process, like X-ray and neutron diffraction, are not sensitive to the local structure around Cu ions. The results are compared to long range order probed by *in situ* diffraction measurements performed in a separate experiment. It has been found that additional local structural changes in the orthorhombic phases occur, not linked to any long-range structural transformation.

Experimental

The epitaxial YNBCO films were prepared by high-pressure pure oxygen sputtering technique [15]. Fully oxygenated high quality films deposited on 10×10 mm^2 and 0.5 mm thick $LaAlO_3$ substrates are obtained. The films have been characterised for their superconducting ($T_c = 87$ K, $\Delta T_c = 1$ K and $J_c\,(77\text{ K}) = 2$ MA/cm^2) and structural properties, showing complete c-axis orientation of the film (that was further confirmed by X-ray diffraction) and smooth surfaces in the μm scale. The films show twinned domains with a and b axis oriented along the axes of the cubic substrate. The details of the film preparation and characterisation have been published elsewhere [16]. The surfaces of the films is free from precipitates as shown clearly in Figure 1 where a Scanning Electron Microscopy (SEM) image of a YNBCO sample is shown. The choice of YNBCO films in place of $Y_1Ba_2Cu_3O_7$ is driven by the better surface morphology exhibited by the Nd-rich films as reported in [15].

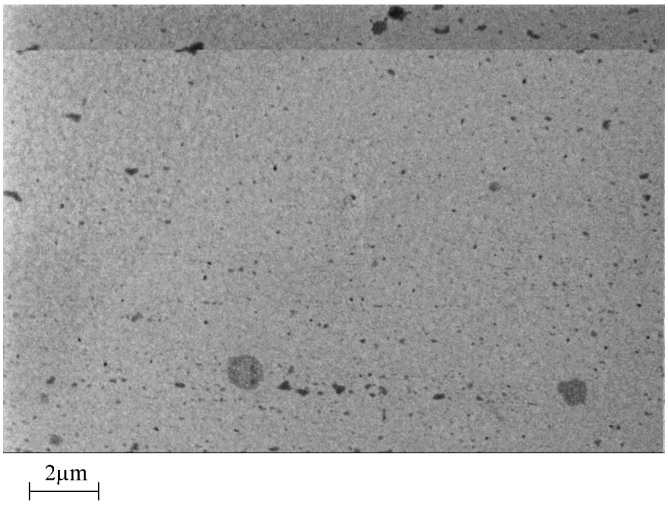

Fig. 1. SEM image of a $Y_1(Nd_{0.05}Ba_{1.95})Cu_3O_x$ thin film showing the absence of second phase precipitates on the surface.

The XAS measurements have been made in the reflection mode using grazing incidence geometry to enhance the contribution of the thin film (thickness ∼150 nm), that allows us to avoid spurious effects due to the sample substrate. Cu K-edge (∼9 KeV) time resolved XANES measurements have been performed at the Dispersive EXAFS beamline ID24, at the European Synchrotron Radiation Facility (ESRF) in Grenoble. The ring was working at $2 \times 1/3$ filling mode, providing an average current of ∼180 mA. The focal spot on the sample position has been measured to be 40 μm $\times$ 200 μm ($H \times V$). This is achieved thanks to the combined effect of the undulator source, the horizontally and vertically demagnifying second and first mirrors respectively, and the profiled dynamically bent Bragg crystal polychromator. This configuration allows the simultaneous acquisition of a whole energy spectra (parallel data acquisition). Finally a third Pt-coated, dynamically bent Si mirror, placed at 0.3 m before the sample, was used for the first time to reduce the vertical focus spot to ∼40 μm, allowing us to perform time resolved experiment on thin films, acquired in reflection mode.

An energy range of ∼400 eV was measured at the second harmonic of the Cu K-edge. Copper thin film, of the same size of the YNBCO sample of interest, has been measured for the energy calibration.

The YNBCO sample was mounted on a heater in a vacuum chamber placed on a two-axis goniometer for the sample alignment. The films were reduced by a high temperature treatment at a heater temperature of 570 °C (about 60 °C higher than the sample temperature) in a pressure of 10^{-5} torr. This process leads to the decreasing of the oxygen content from $x \sim 7.0$ to $x < 6.3$ (tetragonal phase) as confirmed by X-ray diffraction measurements performed on a identical sample prior to the experiment. The annealing step in vacuum is essential for such experiment that requires a mirror-like surface, because allows the evaporations of the contaminants on the surface. Successively the films were cooled down to about 500 °C (corresponding to about 440 °C of the sample) and the oxygenation was promoted by introducing pure oxygen (at the pressure of 600 torr) in the sample chamber. The temperature and the oxygen pressure were kept constant during the oxygenation. We have checked that this process does not modify significantly the structural and superconducting properties of an identical YNBCO film used for test. The grazing incidence angle ($\alpha \sim 0.4$ degree) was chosen so that the penetration depth of the incoming beam was lower than the sample thickness. A position sensitive detector (CCD camera) was used for the parallel data detection. The intensities of the incoming and outcoming beams (I_0 and I_1) were measured at the sample position by detecting the direct (empty) and reflected beams respectively. The optimal acquisition time for each spectrum was found to be equal to 17.5 s for the sample and ~250 ms for the empty beam. The total acquisition time was ~4100 s, *i.e.* 230 spectra were recorded for the oxygenation.

The *in situ* X-ray diffraction experiment has been performed using a conventional Cu Kα θ-2θ diffractometer. The sample can be mounted inside a chamber furnace. The chamber can be evacuated and eventually filled with a controlled (Ar, O_2) atmosphere while the temperature can be raised from 20 °C to a maximum of 1000 °C. The as grown superconducting YNBCO sample is mounted at room temperature. The oxygen is removed from the sample by heating the furnace to 550 °C (at a rate of 50 °C/mn) in a continuous flow of Ar gas maintaining the pressure at about 1.4 mbar. The reduced sample is then cooled to 420 °C in the same atmosphere. Finally the chamber has been filled by 600 mbar of oxygen gas. Since then 30 X-ray θ-2θ spectra around the (006) films and the (200) substrate reflections have been collected during the oxygenation process (2 minutes for each scan). Few spectra have been recorded before the introduction of oxygen gas when the sample was tetragonal. The c-axis of the film is extracted from the position of the (006) peak. Any possible systematic error due, for example, to changes of the diffraction conditions are simple avoided by recording the reference position of the substrate (200) reflection. The c-axis and the corresponding uncertainty in the measured c-axis is determined fitting the data using a Lorentian profile.

Data analysis

In Figure 2 the sample reflectivity measured as a function of energy across the Cu K-edge 4130 s after the beginning of the oxygenation is shown. The spectrum shows different absorption features for the YNBCO system. The absorption features above the threshold are well interpreted due to multiple scattering resonance of the excited photoelectrons scattered by the neighbouring atoms in the continuum part of the spectrum. For example, the main peak B (8.998 KeV) is due to scattering in the basal plane and represent multiple scattering involving mainly the in-plane oxygen atoms. The peaks A_1 (8.986 KeV) and A_2 (8.992 KeV) in the spectrum involve scattering mainly due to the Ba/Y/Nd atoms and the out-of-plane oxygen due to distortions. The details on the origin of the multiple scattering features could be found elsewhere [17–19]. Here it is enough to state that, since the multiple scattering are sensitive to the local geometry, any change in the local atomic displacements within a cluster of radius of ~5 Å around the Cu site are reflected directly by changes in the absorption peaks. Since the film was positioned with the c-axis perpendicular to the polarisation plane of the incident synchrotron beam, the measurements reported in this work are selective to the local structural modifications in the ab plane.

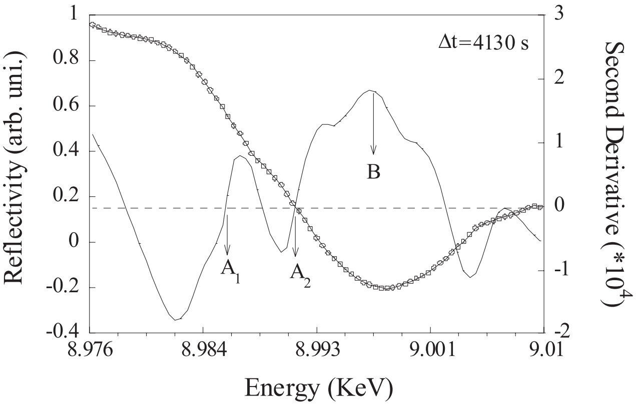

Fig. 2. Cu K-edge XANES reflectivity spectrum of $Y1(Nd_{0.05}Ba_{1.95})Cu_3O_x$ thin film. The second derivative is also shown.

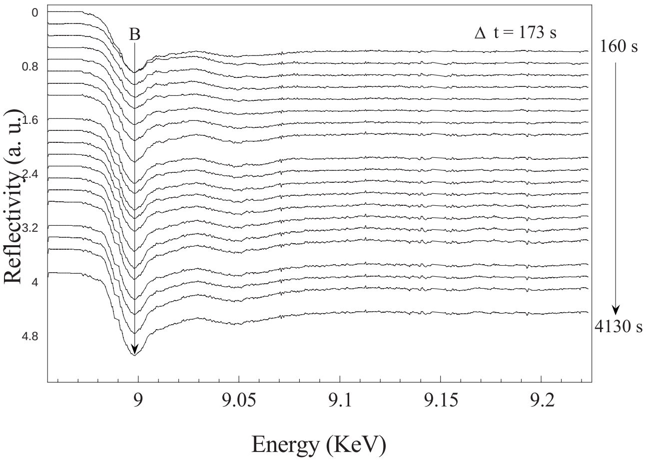

Fig. 3. Reflectivity spectra taken during the oxidation process of $Y_1(Nd_{0.05}Ba_{1.95})Cu_3O_x$. The measurements are shown each 10th spectrum with a Δt between two shown spectra of 173 s.

Figure 3 shows a series of normalised reflectivity spectra taken during the oxidation process of $Y_1(Nd_{0.05}Ba_{1.95})Cu_3O_x$ film. The entire oxidation process has been covered by 230 spectra with each one taking 17.3 sec. We have shown each 10th spectrum for simplicity, resulting in a time interval $\Delta t = 173$ s between each spectra shown in the figure.

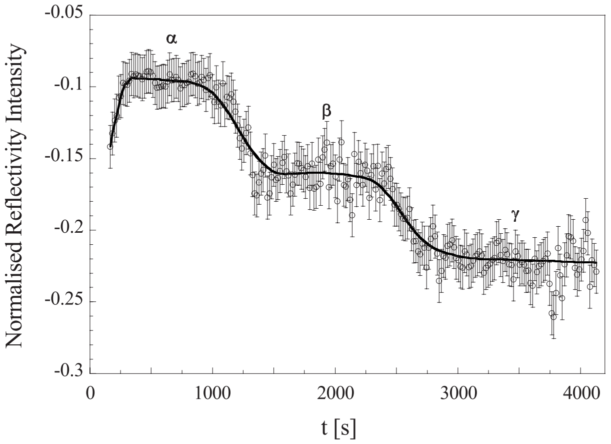

Fig. 4. Temporal evolution of the reflectivity intensity of the B peak defined in Figure 2.

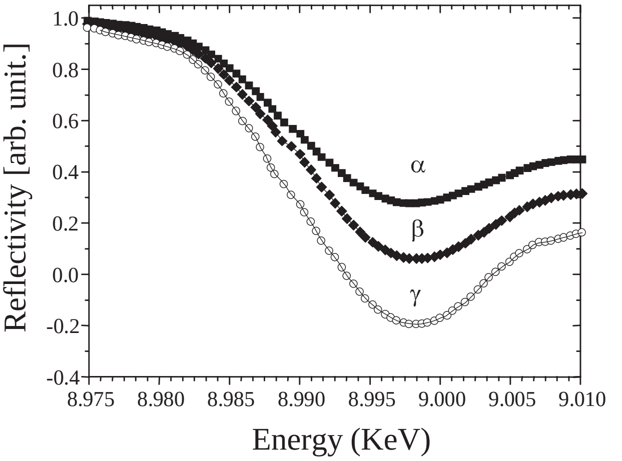

Fig. 5. Comparison between spectra taken at α, β, and γ plateau.

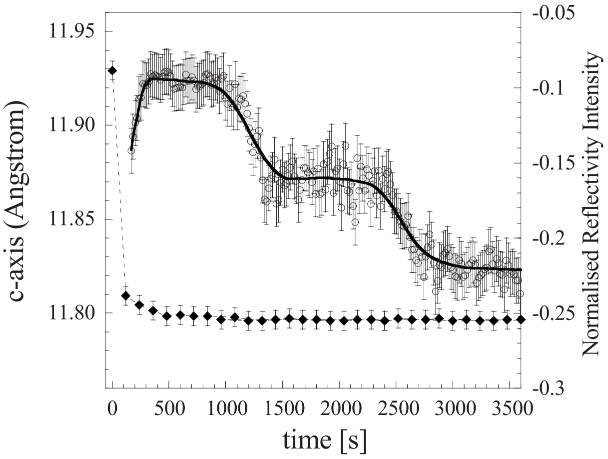

Fig. 6. Temporal evolution of the reflectivity intensity of the peak B plotted together with the c-axis measured in a parallel experiment (closed circles).

To explore the time dependent changes in the local and instantaneous atomic displacements, we have given a systematic look to the absorption peak intensities. Here we focus on the evolution of the main peak B, characteristic of local lattice displacements in the CuO_2 plane. The choice of the peak B is also due to the fact that oxidation process of the RBCO system introduces charge carriers in the CuO_2 plane, which in turn gives superconductivity. In fact, oxidation process is expected influence directly the local electronic and local atomic displacements in the CuO_2 plane. The time dependence of the reflectivity peak B is shown in Figure 4. Each data point is the result of an average over 5 consecutive points, centred on the B position defined by maximum in the second derivative of the reflectivity spectrum (Fig. 2). The error bars represent a mean standard deviation associated to the peak intensity.

The peak intensity shows a decrease with non-linear behaviour as a function of oxidation process (oxygenation time). This happens due to the structural changes within the CuO_2 plane, which involves changes in the Cu-O bonds and Cu-O-Cu buckling angle [20,21]. We can define at least two clear drops representing respectively the transitions from state α to β and β to γ, accompanied by the plateau regions α to β and γ. In addition, a clear increase in the peak intensity appears as soon as the oxidation process starts. In order to interpret the changes in the local environment during oxygenation process, in Figure 5 we plot together three spectra each corresponding to a plateau. It is worth mentioning that we have not measured a XANES absorption spectra, which could be easily compared to many of the results present in literature concerning YBCO samples. Therefore no direct quantitative comparison with other experiments can be performed. Moreover the resolution of the spectra does not allow a clear identification of the local structure around the copper ions. Poor resolution is related to the need to follow the process in time. A typical high-resolution spectrum in our apparatus requires at least 15 minutes, which is too time-expensive. For this reason no definitive conclusion can be drawn relative to the exact structure of the film during the process. However it should be mentioned that the trend of the spectra give meaningful information about the change in the local environment. Here we are interested to the qualitative changes in the spectra, which can be ascribed to in plane local structural modifications around Cu ions. A more definitive picture can be extracted by the comparison of XAS results with the long-range structural information obtained by X-ray diffraction. For this purpose in Figure 6 we plot together the time evolution of the peak intensity (peak B) in the XAS spectra with the c-axis of the film measured during the oxidation process. Obviously in an ideal experiment the structural long-range order and the local order should be measured together. This is very difficult to achieve in a single experiment and for this reason we compare the results from two different experiments. Nevertheless we think that the comparison is meaningful even if very small deviation in the starting oxygen content and sample properties cannot be excluded.

X-ray diffraction shows that starting from a c-axis of 1.195 nm (at 420 °C) typical of the tetragonal phase a quick drop related to the Tetragonal to Orthorhombic Transition is observed. This correlates quite clearly with the quick increase in the main peak before the plateau α is reached. Therefore oxygen enter the film very quickly for this range of temperature and pressure in perfectly agreement with other measurements, like *in situ* conductivity [22] and ellipsometry studies [23]. After only 8–10 minutes the c-axis has reached a stable value within the experimental error. According to present understanding the ORTHO I long range order is established after 10 minutes and the oxygen concentration in the sample has reached the value corresponding to a fully oxygenated film. However, as shown in the previous section, after 10 minutes the sample exhibits a XAS spectra corresponding to the α plateau, and it turns out that at least other two metastable local structures are formed when the c-axis has reached an almost constant value (within the resolution). It is worth mentioning that during the Tetragonal to Orthorhombic crystallographic transition the evolution of the XAFS spectra is related to the change of the structure and to the change of the oxygen content. On the contrary the local changes from state α to β and β to γ happen when the oxygen content and the overall long-range structure of the ORTHO I structure is reached. The results obtained are indicative of a very interesting process occurring in YBCO films upon oxygenation. Indeed even if the tetragonal to orthorhombic transition is very quick and the long range order structure of the film is almost constant after few minutes, in the orthorhombic phase there is an evolution of the local environment of copper as seen by XAFS. In particular only after 40 minutes the spectra typical of an ORTHO I oxygen ordering is observed and at least two local structural transformations are observed before stable ordering is achieved.

The existence of these local structural transformations is very intriguing. We can exclude that the oxygen content in the film changes in an essential way. Therefore the only way to explain the results is by relating different spectra to different ordering of oxygen ions in the CuO planes and/or to transformation in the local CuO_2 structure.

Discussion

It is well known that the ORTHO I structural phase of the RBCO films is realised because the oxygen ions must be introduced in the structure along the b-axis between two Cu ions in the CuO layers. In a fully oxygenated film the O(1) sites along the b-axis are fully occupied, while the O(5) anti-chain sites are empty. To describe the oxygen diffusion and the phase transitions in the YBCO system, standard and modified Antisymmetric Next-Nearest-Neighbor-Ising (ASYNNNI) models have been used in the past with some success. These models are able to simulate stable and metastable oxygen ordering phases supposing that oxygen diffusion proceeds through hopping of oxygen ions to empty sites in the CuO layers. O(1) (chain site)-O(5) (anti-chain site), O(5)-O(5), and O(1)-O(1) hopping mechanisms have been generally considered. Many experimental and theoretical studies have been concentrated on the region of intermediate doping, where besides the ORTHO II phase, other ordered phases like ORTHO III have been effectively observed in bulk and single crystals samples [24]. The amounts of information present in literature concerning diffusion and ordering of oxygen ions for high concentration of oxygen, near the optimally-overdoped phase, are practically absent. Indeed no ordered phase, different from the ordered chain ORTHO I structure, have either been observed or simulated in this region of the phase diagram. It is worth mentioning that these theoretical approaches does not consider the role on the phase diagram of structural changes occurring in the CuO_2 layers, which are on the contrary very important for understanding the superconductivity in this compounds. For example some reports show an experimental correlation between doping, critical temperature and Cu-O-Cu bucking angle [25] in the CuO_2 planes.

Our results show that two other metastable configurations are formed during the oxygenation process of YBCO films. The local nature of oxygen ordering is demonstrated by the lack of a change in the intensity of the (006) reflection and of the corresponding c-axis value, within the resolution of standard X-ray diffraction. Obviously our long-range order information are not complete, since we measure only the c-axis of the film. Therefore we cannot exclude that fine structural effect could indeed be observed. However such analysis requires the acquisition of many reflections, which is at odds with the need to follow the process in time.

While our XAFS spectra are not able to resolve exactly the structural modification which determine the differences between the plateau α, β and γ, it is quite clear that those differences are related to modification within the CuO_2 planes and to smaller extent within the CuO chain layer. Indeed the main difference between the various spectra is the increase of the absorption peak B (decrease in the reflectivity) which indicates changes occurring within the CuO and CuO_2 planes as stated above. We can therefore have two different possible effects which at least qualitatively can explain the increase in the peak B: a) changes of oxygen ordering within the CuO(1) planes; b) changes of the Cu-O-Cu buckling angle and other structural changes in the CuO_2 planes. In YBCO the buckling-angle is modified by doping and by application of a hydrostatic pressure. Roughly increasing the doping and the pressure lead to an increase of the buckling angle [26]. The contribution to the absorption peak of the CuO chain layers can be detected only if a substantial change in the oxygen ordering driven by oxygen content changes takes place. Therefore the main effects leading to the local transformations are structural modifications within the CuO_2 plane. In this respect our observation can be explained by a mechanism similar to the structural displacive transformation observed by EXAFS on YBCO single crystals when the oxygen content is modified from 6.9 to about 7.0 [27]. In [27] it has been shown that in the ORTHO I phase, YBCO undergoes two different local structural transformations involving the changes of the Y-Cu(2) and Y-O(2,3) bond lengths and therefore the changes in the

Cu-O-Cu buckling angle. Our data can be explained in the same way, with the difference that the results shown in [27] are obtained by EXAFS measurements performed on YBCO crystals having different equilibrated oxygen content, while our data concern the *in situ* study of the oxygenation process. This result, if confirmed by accurate time resolved EXAFS measurements, show that the oxygenation process of YBCO films is not trivial, and depending on the process, samples having substantial structurally different CuO_2 planes can be grown even maintaining the same apparent oxygen content and overall structure. It should be mentioned that in [27] the structural transformations in YBCO are correlated to the passage from the underdoped to overdoped phase, where strange and important phenomena, like phase separation, can occur due to the passage from a correlated strange metal to an almost Fermi liquid material. From this point of view our results are in some sense surprising because it turns out that our YNBCO films are underdoped because Nd excess decreases the overall number of carrier in the CuO_2 planes. We have measured on YNBCO films roughly about $n = 2 \times 10^{21}$ holes cm^{-3} through Hall effect and thermoelectric effect measurements. Consequently the local transformations observed in our films are not correlated to the passage from an underdoped to an overdoped phase, as apparently happens instead in YBCO. This points merit further investigations in order to understand if the displacive transformation in YBCO are or not related to the passage from the underdoped to the overdoped phase.

In summary, we have exploited time resolved X-ray absorption spectroscopy to study evolution of the local displacements in the RBCO system due to the oxygen insertion in the Cu-O chain. Epitaxial thin films of superconducting $Y_1(Nd_{0.05}Ba_{1.95})Cu_3O_x$ are studied by Cu K-edge XANES, performed in the dispersive geometry in reflection mode. To the best of our knowledge, the time resolved X-ray absorption spectroscopy has been used for the first time to study the local structure in the oxidation process of the REBCO compounds in form of thin films. The reflectivity spectrum shows an interesting time evolution with step-like changes, revealed by the time dependence of the main peak intensity. After the film has reached the ORTHO I long range order as revealed by X-ray diffraction, two local structural transitions are observed around the Cu ions in the ab plane of the film. The correlation between X-ray diffraction and XAFS reveals that these transitions can be assigned to displacive transformations within the CuO_2 plane, in analogy with what happen in the case of YBCO changing the oxygen content from 6.9 (underdoped phase) to 7.0 (overdoped phase). In our case the film remains underdoped due to the excess of Nd at Ba site, revealing that displacive transformation in our case are not related to the underdoping-overdoping transition.

Our results show that YBCO film oxygenation is not trivial and not fully understood process, since different CuO_2 structures can be frozen depending on the procedure used, even when the long range structure and the oxygen content appear to be identical.

The authors are glad to thank the ID24 beamline staff for their help and co-operation during the experimental run. We thank Dr. M. Putti for the Hall effect measurements on our films.

References

1. H.J. Sheel, M. Berkowski, B. Chabot, J. Cryst. Growth **115**, 19 (1991)
2. H.J. Sheel, MRS Bulletin **19**, 26 (1994)
3. M.J. Kramer, S.I. Yoo, R.W. McCallum, W.B. Yelon, H. Xie, P. Allenspach, Physica C (Amsterdam) **219**, 145 (1994)
4. T. Ito, K. Takenaka, S. Uchida, Phys. Rev. Lett. **70**, 3995 (1993)
5. J. Ye, K. Nakamura, Phys. Rev. B **48**, 7554 (1993)
6. H. Küpfer, Th. Wolf, C. Lessing, A.A. Zhukov, X. Lanon, R. Meier-Hirmer, W. Schauer, H. Wühl Phys. Rev. B **58**, 2886 (1998)
7. L. Hou, J. Deak, P. Metcalf, M. McElfresh, G. Preosti, Phys. Rev. B **55**, 11806 (1997)
8. R.D. Hunt, E.C. Beham, G.F. Voronin, Physica C (Amsterdam) **302**, 130 (1998)
9. E. Straube, D. Hohlwein, F. Kubanek, Physica C (Amsterdam) **295**, 1 (1998)
10. M. Kläser, J. Kaiser, F. Stock, G. Müller-Vogt, A. Erb, Physica C (Amsterdam) **306**, 188 (1998)
11. S.J. Rothman, J.L. Routbort, U. Welp, J.E. Baker, Phys. Rev. B **44**, 2326 (1991)
12. S. Kittelberger, U. Bolz, R.P. Huebener, B. Holzapfel, L. Mex, Physica C (Amsterdam) **302**, 93 (1998)
13. P. Manca, S. Sanna, G. Calestani, A. Migliori, R. De Renzi, G. Allodi, Phys. Rev. B **61**, 15450 (2000)
14. R. Mogilevsky, R. Levi-Setti, B. Pashmakov, Li Liu, K. Zhang, H.M. Jaeger, D.B. Buchholz, R.PO.H. Chang, B.W. Veal, Phys Rev. B **49**, 6421 (1994)
15. M. Salluzzo, I. Maggio-Aprile, ∅. Fischer, Appl. Phys. Lett. **73**, 683 (1998)
16. M. Salluzzo *et al.*, IEEE Trans on Appl. Supercond. **11**, 3201 (2001)
17. A. Bianconi, C. Li, F. Campanella, S. Della Longa, I. Pettiti, M. Pompa, S. Turtu, D. Udron, Phys. Rev. B **44**, 4560 (1991)
18. N.L. Saini, A. Lanzara, A. Bianconi, H. Oyanagi, Phys. Rev. B **58**, 11768 (1998)
19. N.L. Saini, A. Lanzara, F. Natali, A. Bianconi, M. Akoshima, Y. Koike, H. Oyanagi, J. Synchrotron Rad. **6**, 752 (1999)
20. H. Shaked, J.D. Jorgensen, D.G. Hinks, R.L. Hitterman, B. Dabrowski, Physica C (Amsterdam) **205**, 225 (1993)
21. J.D. Jorgensen, M.A. Beno, D.G. Hinks, L. Soderholm, K.J. Volin, R.L. Hitterman, J.D. Grace, I.K. Schuller, C.U. Segre, K. Zhang, M.S. Kleefisch, Phys. Rev. B **36**, 7, 3608 (1987)
22. V. Dediu, F.C. Matacotta, Phys. Rev. B **54**, 16259 (1996)
23. A. Michaelis, E.A. Irene, O. Auciello, A.R. Krauss, J. Appl. Phys. **83**, 7736 (1998)
24. M. Ausloos, A. Pekalski, Phys. Rev. B **52**, 4577 (1995)
25. O. Chmaissem, J.D. Jorgensen, S. Short, A. Knizhnik, Y. Eckstein, H. Shaked, Nature **397**, 45 (1999)
26. A. Sahiner, E.D. Crozier, D.T. Jiang, R. Ingalls, Phys. Rev. B **59**, 3902 (1999)
27. E. Kaldis, J. Röhler, E. Liarokapis, N. Poulakis, K. Conder, P.W. Loeffen, Phys. Rev. Lett. **79**, 4894 (1997)